Supplementary Information

Stability of the Antarctic Ice Sheet during the pre-Industrial Holocene

Authors: Richard S. Jones[1,2†], Joanne S. Johnson[3], Yucheng Lin[4], Andrew N. Mackintosh[1,2], Juliet P. Sefton[5], James A. Smith[3], Elizabeth R. Thomas[3] and Pippa L. Whitehouse[4]

Affiliations: [1] Earth Atmosphere and Environment, Monash University, Clayton, Victoria, Australia. [2] Securing Antarctica's Environmental Future, Monash University, Clayton, Victoria, Australia. [3] British Antarctic Survey, Cambridge, U.K. [4] Department of Geography, Durham University, Durham, U.K. [5] Earth and Ocean Sciences, Tufts University, Medford, MA, U.S.A.

[†]*email: richard.s.jones@monash.edu*

SUPPLEMENTARY METHODS

Empirical evidence of Antarctic Ice Sheet change

Empirical evidence was utilised to support the findings and interpretations of published literature, and to help visualise patterns of Antarctic Ice Sheet change during the Holocene. The data were sourced from databases, review paper compilations and original publications, and were analysed systematically where possible. To provide a spatial evaluation of ice sheet change through the Holocene, the empirical data were divided into ice sheet sectors, based on modern ice divides[1] that were extrapolated to the continental shelf edge: Antarctic Peninsula, Weddell Sea, East Antarctica, Ross Sea and Amundsen Sea. The datasets assessed in this review, and the code used to analyse and plot the data are available at https://github.com/rs-jones/antarctica-holocene, and the figures used cmocean colormaps[2].

Cosmogenic exposure data

Ice thickness change near the ice sheet margins was assessed using cosmogenic exposure data (Box 1). These data were sourced from the ICE-D Antarctica database (http://antarctica.ice-d.org/; accessed 05 November 2021), which provides an up-to-date compilation of sample information and exposure ages. The database uses its own framework to categorise and calculate exposure ages based on the contained sample information, and updates the exposure ages every 24 hours using the most recent developments in the calculation process[3].

To prioritise data that should provide a reliable timeline of ice thickness change, data were included only where the site was categorised as a nunatak, with a minimum of 5 samples covering at least 10 m elevation range. Cosmogenic inheritance from insufficient erosion of the surface during periods of ice cover can result in erroneously old exposure ages[4], however, this should be minimal during the Holocene. The exposure ages utilised here were from the most commonly-applied isotope (^{10}Be) and the isotope with the smallest inheritance signal (^{14}C), calculated using the LSDn scaling scheme[5]. While the *in situ*-produced cosmogenic ^{14}C ages should provide a more

reliable estimate for the timing of ice thickness change, especially prior to the Holocene[6], there are currently too few records to allow for a widespread assessment of Antarctic Ice Sheet change solely using *in-situ* ^{14}C data.

These cosmogenic exposure data were used to produce Figure 2a. The probability density functions are kernel density estimates[7], which were calculated for each exposure age from the mean and standard deviation, and summed for each sector. The rate of ice surface elevation change was estimated by linearly interpolating the age-elevation data at each site, calculating the elevation difference for 1000-year windows, and averaging across sites for each sector.

Snow accumulation rate data

Ice thickness change in the interior was assessed using the rate of snow accumulation from ice core records. It is currently challenging to estimate absolute ice thickness change from ice cores. However, snow accumulation provides a useful indicator of ice thinning or thickening at a site as it is the primary control on ice surface elevation change[8] (Box 1). The accumulation rates and age chronologies were taken from a recent compilation of Antarctic ice core records[9]. While there are many more records of snow accumulation from ice cores, particularly during the Late Holocene[10], records that span the full length of the Holocene were prioritised for this review.

These data were used to produce Figure 2b. To help visualise the inferred change in ice thickness at each ice core, the accumulation rates were summed for 500-year windows, and plotted relative to pre-Industrial (1700-1850 CE). For WAIS Divide, Dome C and Dome Fuji, the corresponding change in ice surface elevation has been estimated from modelling of the accumulation rate and ice flow, which is shown in Figure 2b as published in the original studies[11,12].

Grounding line retreat data

The timing of grounding line retreat was assessed using published chronologies. Ages that directly constrain the retreat of grounded ice were prioritised (Box 1), opposed to relative changes in the grounding line position (i.e., distal to proximal) or retreat of the ice shelf margin. In a limited number of cases (for example, to capture inland retreat in the Siple Coast region[13]), we included a broad age-range for grounding line retreat. Since the reliability of a retreat age is dependent on the geological setting of the site, marine radiocarbon approach (e.g. calcareous microfossils, bulk, compound specific, ramped pyrolysis) and correction method (e.g. marine reservoir effect with appropriate ΔR)[14–16], this review used the most recently published age estimate for each record, and only records that have been previously assessed as reliable estimates of grounding line retreat. For records published before 2014, ages were taken from the RAISED Consortium suite of reviews[17–21]. For records published from 2014 onwards, ages were taken from the original study, which typically followed a framework for determining reliability and calculating ages as recommended by the RAISED Consortium.

These data were used to produce Figure 3. In Figure 3b, the probability density functions are kernel density estimates (as produced for the cosmogenic exposure data), which were calculated for each retreat age from the mid-age and standard deviation, and summed for each sector.

Relative sea level data

Ice mass change in coastal locations was assessed from records of relative sea level change, which reflect the solid-Earth response to regional ice mass gain and loss (Box 1). Due to the complexities in interpreting and visualising the response to ice mass change from relative sea level change, these data are not compiled and analysed in this review. Instead, the timings of ice mass gain and loss are presented in Figure 3 based on the published interpretations of the relative sea level records and the most recently calculated ages of the changes.

Sea level modelling

Sea level modelling was carried out using a gravitationally self-consistent theory that accounts for shoreline migration and rotational feedback[22–24].

Two primary inputs must be defined in the model: the rheological properties of the solid Earth and the ice loading history. The solid Earth was represented using a spherically-symmetric, depth-varying (i.e., 1-D), self-gravitating Maxwell body, which comprises an elastic lithosphere, and an upper and lower mantle extending to 670 km and from 670 km to the core-mantle boundary, respectively. The elastic and density structure of the Earth was derived from the preliminary reference Earth model[25]. The Earth models were created by combining two effective lithospheric thicknesses (71 and 96 km) with four upper mantle viscosities (0.1, 0.3, 0.8, 1×10^{21} Pa s) and three lower mantle viscosities (5, 10, 30×10^{21} Pa s). The ice loading history describes Holocene change across Antarctica, and was taken from the 11 published ice models presented in Figure 4[26–34]. In total, a suite of 264 model combinations were tested, consisting of 24 Earth and 11 ice models.

For this review, the focus is the modelled spatial pattern of sea-level change and global mean sea-level contribution from Antarctic ice volume change during the Holocene. Figure 6 shows the spatially variable patterns of sea-level change for a) a period of modelled rapid ice loss (12,000 to 8,000 years ago), which uses the mean of the 11 ice models, and b) a scenario of ice volume gain (3,000 to 0 years ago), which uses a single ice model with the greatest ice sheet readvance. In both cases, the mean and standard deviation from the 24 Earth models was calculated across the 11 ice models or for the single ice model, respectively. Supplementary Figure S1 shows an alternative scenario of ice gain, which instead uses the ice model with the greatest total ice volume gain (5,000 to 0 years ago) as opposed to the greatest readvance. The Antarctic contribution to global mean sea-level (which excludes the contribution from ice below flotation) was calculated for the 11 ice models, taking the mean of the 24 Earth models, and is shown in Supplementary Table S1.

SUPPLEMENTARY TABLES

Table S1. Global mean sea level contribution from Antarctica during the Holocene (metres); values indicate global mean sea level at each time, relative to present.

Ice model	Time (thousand years ago)									
	12	10	9	8	7	6	5	4	2	0
A20	11.98	12.32	11.88	9.23	6.23	3.24	0.43	-0.19	-0.22	0.00
B14	5.47	2.20	1.43	0.80	0.60	0.44	0.24	0.17	0.02	0.00
G14	6.45	3.26	2.16	1.33	1.19	0.98	0.74	0.59	0.39	0.00
G20ig5	2.52	1.01	0.49	0.27	0.12	0.10	0.03	0.02	-0.03	0.00
G20anu	5.61	3.80	2.25	1.61	1.25	1.06	0.75	0.53	0.21	0.00
P18	4.04	1.75	0.96	0.60	0.44	0.26	0.06	0.07	-0.01	0.00
P17elra	5.53	2.96	1.97	1.43	1.13	0.90	0.67	0.58	0.28	0.00
P17st	5.19	3.49	1.84	0.83	0.44	0.21	0.11	0.16	-0.03	0.00
T18	8.93	4.35	2.62	1.81	1.35	1.00	0.77	0.44	-0.09	0.00
W12	2.33	1.55	0.89	0.36	-0.08	-0.48	-0.87	-0.71	-0.36	0.00
K18	4.93	1.60	0.82	0.50	0.29	0.07	0.01	-0.07	-0.19	0.00

SUPPLEMENTARY FIGURES

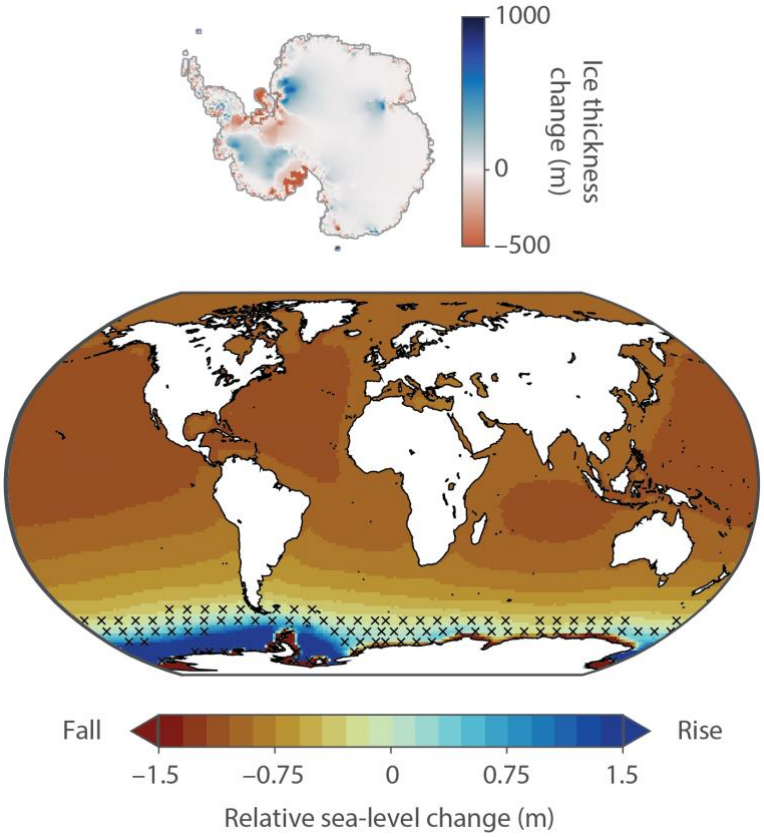

Figure S1. Pattern of global sea-level change due to a scenario of Antarctic ice volume gain. The maps show simulated ice thickness change and corresponding modelled relative sea-level change, akin to Figure 6b. Here, however, the ice sheet model with the greatest Mid-to-Late Holocene ice volume gain[31] (W12 in Supplementary Table S1), rather than greatest readvance (K18), is used. Ice gain in this model comes from interior thickening, despite continued grounding-line retreat, and is simulated between 5,000 years ago and present (note, the time period is different to Figure 6b). Sea-level fall (up to 1.2 m) is predicted in the north and central Pacific Ocean, north Atlantic Ocean, and Indian Ocean. Meanwhile, sea-level rise is predicted in the Southern Ocean, in the vicinity of the Antarctic Peninsula, Weddell Sea and Amundsen Sea sectors.

REFERENCES

1. Mouginot, J., Scheuchl, B. & Rignot, E. MEaSURES Antarctic Boundaries for IPY 2007-2009 from Satellite Radar, Version 2. (2017) doi:10.5067/AXE4121732AD.
2. Thyng, K. M., Greene, C. A., Hetland, R. D., Zimmerle, H. M. & DiMarco, S. F. True colors of oceanography: Guidelines for effective and accurate colormap selection. *Oceanography* **29**, 9–13 (2016).
3. Balco, G. Technical note: A prototype transparent-middle-layer data management and analysis infrastructure for cosmogenic-nuclide exposure dating. *Geochronology* **2**, 169–175 (2020).
4. Balco, G. Glacier Change and Paleoclimate Applications of Cosmogenic-Nuclide Exposure Dating. *Annu. Rev. Earth Planet. Sci.* **48**, 21–48 (2020).
5. Lifton, N., Sato, T. & Dunai, T. J. Scaling in situ cosmogenic nuclide production rates using analytical approximations to atmospheric cosmic-ray fluxes. *Earth Planet. Sci. Lett.* **386**, 149–160 (2014).
6. Nichols, K. A. *et al.* New Last Glacial Maximum ice thickness constraints for the Weddell Sea Embayment, Antarctica. *The Cryosphere* **13**, 2935–2951 (2019).
7. Jones, R., Small, D., Cahill, N., Bentley, M. & Whitehouse, P. iceTEA: Tools for plotting and analysing cosmogenic-nuclide surface-exposure data from former ice margins. *Quat. Geochronol.* **51**, 72–86 (2019).
8. Helsen, M. M. *et al.* Elevation Changes in Antarctica Mainly Determined by Accumulation Variability. *Science* **320**, 1626–1629 (2008).
9. Buizert, C. *et al.* Antarctic surface temperature and elevation during the Last Glacial Maximum. *Science* **372**, 1097–1101 (2021).
10. Thomas, E. R. *et al.* Regional Antarctic snow accumulation over the past 1000 years. *Clim. Past* **13**, 1491–1513 (2017).
11. Parrenin, F. *et al.* 1-D-ice flow modelling at EPICA Dome C and Dome Fuji, East Antarctica. *Clim. Past* **3**, 243–259 (2007).
12. Koutnik, M. R. *et al.* Holocene accumulation and ice flow near the West Antarctic Ice Sheet Divide ice core site. *J. Geophys. Res. Earth Surf.* **121**, 907–924 (2016).
13. Venturelli, R. A. *et al.* Mid-Holocene Grounding Line Retreat and Readvance at Whillans Ice Stream, West Antarctica. *Geophys. Res. Lett.* **47**, e2020GL088476 (2020).
14. Prothro, L. O. *et al.* Timing and pathways of East Antarctic Ice Sheet retreat. *Quat. Sci. Rev.* **230**, 106166 (2020).
15. Bart, P. J., DeCesare, M., Rosenheim, B. E., Majewski, W. & McGlannan, A. A centuries-long delay between a paleo-ice-shelf collapse and grounding-line retreat in the Whales Deep Basin, eastern Ross Sea, Antarctica. *Sci. Rep.* **8**, 12392 (2018).
16. Subt, C., Fangman, K. A., Wellner, J. S. & Rosenheim, B. E. Sediment chronology in Antarctic deglacial sediments: Reconciling organic carbon 14C ages to carbonate 14C ages using Ramped PyrOx. *The Holocene* **26**, 265–273 (2016).
17. Cofaigh, C. Ó. *et al.* Reconstruction of ice-sheet changes in the Antarctic Peninsula since the Last Glacial Maximum. *Quat. Sci. Rev.* **100**, 87–110 (2014).
18. Hillenbrand, C.-D. *et al.* Reconstruction of changes in the Weddell Sea sector of the Antarctic Ice Sheet since the Last Glacial Maximum. *Quat. Sci. Rev.* **100**, 111–136 (2014).
19. Mackintosh, A. N. *et al.* Retreat history of the East Antarctic Ice Sheet since the Last Glacial Maximum. *Quat. Sci. Rev.* **100**, 10–30 (2014).
20. Anderson, J. B. *et al.* Ross Sea paleo-ice sheet drainage and deglacial history during and since the LGM. *Quat. Sci. Rev.* **100**, 31–54 (2014).

21. Larter, R. D. *et al.* Reconstruction of changes in the Amundsen Sea and Bellingshausen Sea sector of the West Antarctic Ice Sheet since the Last Glacial Maximum. *Quat. Sci. Rev.* **100**, 55–86 (2014).
22. Kendall, R. A., Mitrovica, J. X. & Milne, G. A. On post-glacial sea level – II. Numerical formulation and comparative results on spherically symmetric models. *Geophys. J. Int.* **161**, 679–706 (2005).
23. Mitrovica, J. X., Wahr, J., Matsuyama, I. & Paulson, A. The rotational stability of an ice-age earth. *Geophys. J. Int.* **161**, 491–506 (2005).
24. Milne, G., A. & Mitrovica, J., X. Postglacial sea-level change on a rotating Earth. *Geophys. J. Int.* **133**, 1–19 (1998).
25. Dziewonski, A. M. & Anderson, D. L. Preliminary reference Earth model. *Phys. Earth Planet. Inter.* **25**, 297–356 (1981).
26. Golledge, N. R. *et al.* Antarctic contribution to meltwater pulse 1A from reduced Southern Ocean overturning. *Nat. Commun.* **5**, 1–10 (2014).
27. Pollard, D., Gomez, N., DeConto, R. & Han, H. Estimating Modern Elevations of Pliocene Shorelines Using a Coupled Ice Sheet-Earth-Sea Level Model. *J. Geophys. Res. Earth Surf.* **123**, 2279–2291 (2018).
28. Pollard, D., Gomez, N. & Deconto, R. M. Variations of the Antarctic Ice Sheet in a Coupled Ice Sheet-Earth-Sea Level Model: Sensitivity to Viscoelastic Earth Properties. *J. Geophys. Res. Earth Surf.* **122**, 2124–2138 (2017).
29. Kingslake, J. *et al.* Extensive retreat and re-advance of the West Antarctic ice sheet during the Holocene. *Nature* **558**, 430–434 (2018).
30. Albrecht, T., Winkelmann, R. & Levermann, A. Glacial-cycle simulations of the Antarctic Ice Sheet with the Parallel Ice Sheet Model (PISM) – Part 2: Parameter ensemble analysis. *The Cryosphere* **14**, 633–656 (2020).
31. Whitehouse, P. L., Bentley, M. J. & Le Brocq, A. M. A deglacial model for Antarctica: geological constraints and glaciological modelling as a basis for a new model of Antarctic glacial isostatic adjustment. *Quat. Sci. Rev.* **32**, 1–24 (2012).
32. Gomez, N., Weber, M. E., Clark, P. U., Mitrovica, J. X. & Han, H. K. Antarctic ice dynamics amplified by Northern Hemisphere sea-level forcing. *Nature* **587**, 600–604 (2020).
33. Tigchelaar, M., Timmermann, A., Friedrich, T., Heinemann, M. & Pollard, D. Nonlinear response of the Antarctic Ice Sheet to late Quaternary sea level and climate forcing. *Cryosphere* **13**, (2019).
34. Briggs, R. D., Pollard, D. & Tarasov, L. A data-constrained large ensemble analysis of Antarctic evolution since the Eemian. *Quat. Sci. Rev.* **103**, 91–115 (2014).